International Communications in Heat and Mass Transfer 116 (2020) 104694

Contents lists available at ScienceDirect

International Communications in Heat and Mass Transfer

journal homepage: www.elsevier.com/locate/ichmt

Machine learning for heat transfer correlations

Beomjin Kwon[a,*], Faizan Ejaz[a], Leslie K. Hwang[b]

[a] School for Engineering of Matter, Transport and Energy, Arizona State University, Tempe, AZ 85287, USA
[b] Sunnyvale, CA 94085, USA

ARTICLE INFO

Keywords:
Heat transfer correlation
Machine learning
Random forests
Variable rib roughness

ABSTRACT

This paper explores machine learning approach as a heat transfer correlation. Machine learning significantly reduces the effort to develop multi-variable heat transfer correlations, and is capable of readily expanding the parameter domain. Random forests algorithm is used to predict the convection heat transfer coefficients for a high-order nonlinear heat transfer problem, i.e., convection in a cooling channel integrated with variable rib roughness. For 243 different rib array geometries, numerical simulations are performed to train and test ML model based on six input features. Machine learning model predicts closely to numerical simulation data with high determination of coefficient (R^2), e.g., $R^2 > 0.966$ for the testing dataset. The capability and limitation of random forests algorithm are discussed with validation dataset.

1. Introduction

Convective heat transfer often manifests in complex physics such that empirical correlations, i.e., mathematical forms that correlate convective heat transfer with surface geometry and flow conditions, are popular means to solve the convection problems [1]. However, if a convective heat transfer is a high-order nonlinear function of many parameters, it becomes challenging to find a mathematical form that achieves high accuracy. For example, channels with rough surfaces such as wavy channels [2], corrugated channels [3], and the channels integrated with internal ribs [4] are widely used in engineering applications where heat transfer augmentation is essential. Surface roughness enhances heat transfer by catalyzing flow separation and mixing, leading to flow instability and nonlinear behaviors. Often, it is extremely difficult to accurately express the heat transfer associated with the surface roughness using simple mathematical forms, which has been prohibitive for modeling such systems.

Recently, machine learning, ML, has been impacting a variety of fields including medicine, health care, robotics, and even scientific research areas [5–9]. For example, in the area of fluid mechanics, ML is used to analyze a large amount of data obtained from experiments, field measurements, and numerical simulations [9–14]. Machine learning based data analysis not only improves the throughput and accuracy of flow interpretation, but also unlocks new opportunities like quantitative predictions of flow properties based on qualitative data [14] or data from past occasions [15].

The area of thermal science and engineering has also been exploring how to facilitate data analysis using ML [16–19]. Recent demonstrations used support-vector machine and neural network algorithms to identify pool boiling regimes [20]. More than 10,000 images for water boiling were used to train the ML models, enabling the algorithm to classify the boiling regime with an accuracy of 99%. When the algorithm learned how to link the water boiling images with a quantitative information, i.e., heat flux, the model was able to predict the heat flux based on the image data [16]. Another demonstration used extreme learning machine algorithm to predict the comfort index of air-conditioned rooms when six input parameters were given [18]. The ML algorithm predicted 16% more accurately than those by a traditional correlation. A previous work compared several ML algorithms as regression models for Nusselt number of helically coiled tube heat exchangers [17]. This work compared multilayer perceptron artificial neural network, adaptive neuro-fuzzy inference system, and support vector machine with 72 data points varied by three input parameters. While previous works show that ML offers considerable promise, the field of ML for heat transfer is yet considered very immature and there remain many unresolved problems.

This article explores how ML can serve as a correlation for high-order nonlinear convection heat transfer. Especially, this study focuses on a cooling channel integrated with variable rib roughness. The ML model is first trained by the numerically simulated data using random forests regressor [21], and predicts the local convective heat transfer coefficient of the cooling channel. Then, the interpolation capability of the RF regression is tested using various new channel geometries.

* Corresponding author.
E-mail address: kwon@asu.edu (B. Kwon).

https://doi.org/10.1016/j.icheatmasstransfer.2020.104694

Available online 25 June 2020

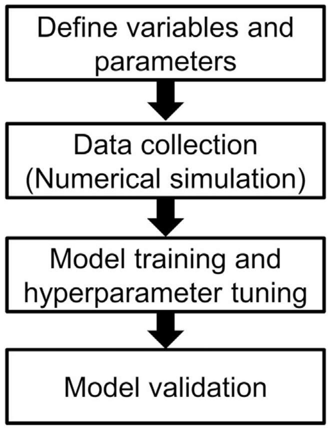

Fig. 1. Flowchart of ML process.

2. Methodology

Fig. 1 illustrates an overall process of training an ML model as a heat transfer correlation. Machine learning algorithms are capable of handling numerous features and rank the importance. However, as the number of features increases, the amount of data and time required for training increases accordingly. Hence, foremost, it is necessary to adequately select which data features, i.e., geometric parameters of fluidic devices or fluid variables, are of interest to the correlation. After the feature selection, data collection follows. For deriving heat transfer correlations, the cost of data preparation can be significant, as data is generated either by experiments or numerical simulations. To minimize the cost and to avoid underfitting issue in ML, the range and spacing of dataset must be well determined. Once the dataset is ready, the collected information is formatted into a two-dimensional numerical matrix, namely feature matrix, as input to the ML algorithm. During the training, tuning of hyperparameters is usually required to enhance the accuracy. Lastly, the obtained ML model is evaluated using data that it is outside of the training dataset. Usually a subset of collected data is used to validate the trained ML algorithm.

3. Data collection and preparation

Fig. 2(a) shows a schematic of two-dimensional rough channel integrated with five ribs, with an arbitrary combination of rib heights. The channels studied in this work have a height, H, of 3 mm and an overall length, L, of 5.5 mm. Ribs have a width of 0.5 mm each and a pitch, p, of 1 mm. For collecting ML data, the height of each rib is varied within three values, i.e., 0.0001, 0.1 or 1 mm. Thus, the number of channel geometries included in ML dataset is $3^5 = 243$. For boundary conditions, the Reynolds number at the inlet is 50 and water is used as coolant in these channels. A constant heat flux, q'', of 1 W/cm^2 is applied at the channel bottom wall along the rib, while channel top wall is adiabatic.

A finite volume model, FVM, was used to simulate the steady-state flow and heat transfer in the rough channels, implemented in a commercial software, ANSYS 19.0. Fig. 2(b) shows the calculated velocity streamlines for one of channel geometries with rib heights, e_n, of $[e_1, e_2, e_3, e_4, e_5] = [1, 0.0001, 0.1, 1, 1]$ (mm), where the subscript n indicates the order of rib from the channel entrance. Ribs cause flow rotations and the boundary layer separation at the leading rib edges. Fig. 2(c) shows the calculated temperature distribution of the same channel. The complex flow topology shown in Fig. 2(b) causes nonlinear, irregular temperature patterns, which are the characteristics of variable rough surfaces. The calculated temperatures of wall, $T_w(x)$, and mean water temperature along x-axis, $T_m(x)$, allow to estimate local convection heat transfer coefficient, $h(x)$, by the relation, $h(x) = q''/[T_w(x) - T_m(x)]$.

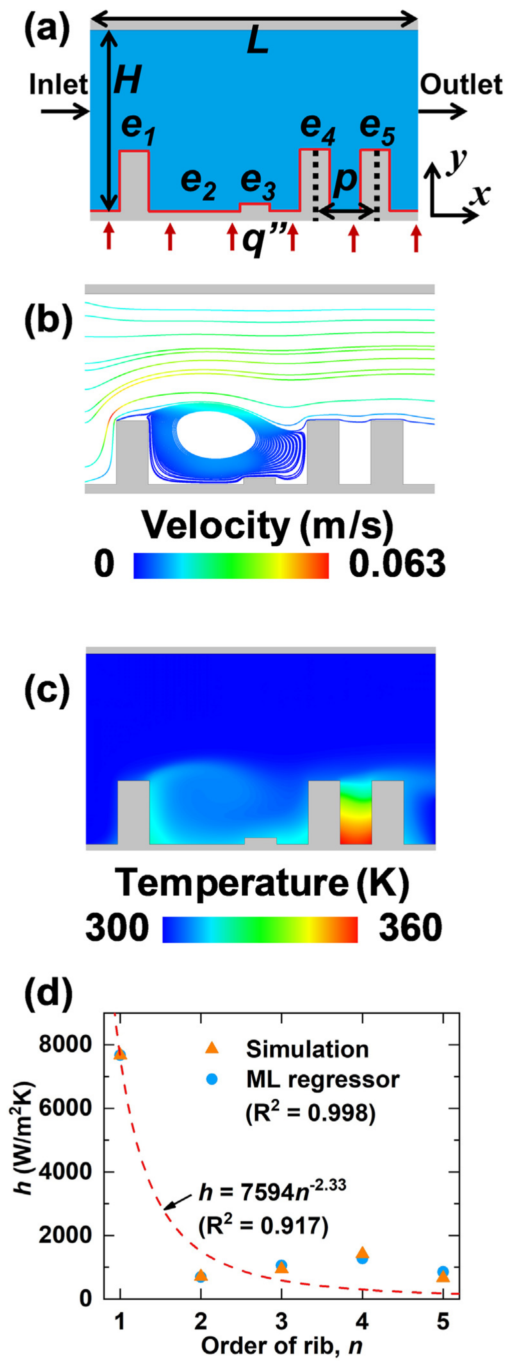

Fig. 2. A side-view schematic of the two-dimensional channel with variable rib roughness. The channel is subject to a uniform heat flux at the bottom wall, indicated by a red line. (b) Velocity streamlines, and (c) temperature map simulated by FVM for the channel geometry with $[e_1, e_2, e_3, e_4, e_5] = [1, 0.0001, 0.1, 1, 1]$ (mm). (d) Convection heat transfer coefficients predicted by both FVM and ML regressor for the channel shown above. (For interpretation of the references to colour in this figure legend, the reader is referred to the web version of this article.)

The calculated $h(x)$ is used to estimate the convection heat transfer coefficient for each rib region, h_n. Due to complex flow and temperature patterns with variable ribs, h_n nonlinearly varies along x direction as shown in Fig. 2(d). Nonlinearity in $h(x)$ prohibits to derive a simple mathematical correlation. However, an ML regressor is able to fit h_n with a high determination of coefficient (R^2), which will be discussed with more details later in the article. A simple power function,

$h = 7594n^{-2.33}$, less accurately fits to the FVM predictions than the ML regressor, indicating that fitting of nonlinearly scattered data is a challenging task.

Using the simulation results of 243 channel geometries, a feature matrix was prepared, consisting of six features, i.e., n and rib heights, to fit five outcome values, i.e., h_n. Then, randomly selected 75% of data were employed for training, and remaining 25% of data were used for testing.

4. Model training and testing

For the data regression, this work particularly uses a general-purpose regressor, random forests (RF) algorithm, implemented in scikit-learn [21,22]. This algorithm operates as an ensemble of several randomized decision trees, and makes decision by averaging the predictions made by the trees. Important hyperparameters for RF include the depth of each tree (denoted as max_depth), seed number used by a random number generator (denoted as random_state), and the number of trees in the forest (denoted as n_estimator). Due to the simplicity of the algorithm and an open-source implementation provided in scikit-learn [22], RF has been one of the popular ML algorithms.

Fig. 3 compares the convection heat transfer coefficients predicted by FVM and RF algorithm. In general, the RF regressor fits h_n closely to FVM predictions of all variable rib geometries with $R^2 > 0.860$ for the training dataset and $R^2 > 0.966$ for the testing dataset. The scores of 5-fold cross validation were also estimated as 0.997 both for training and testing datasets. Note that it has not been possible to fit the heat transfer properties in such a variety of complex channel geometries by using a simple mathematical-form correlation. During training, the most sensitive hyperparameter to affect the accuracy was found to be n_estimator in our study. When n_estimator was 1, R^2 for h_5 data was merely 0.286. However, when n_estimator ≥ 100, R^2 for h_5 increased and saturated to 0.860. Thus, n_estimator of 100 was chosen for all the following ML regression tasks. We varied other hyperparameters such as max_depth ranging 20–100 and random_state ranging 0–100, but these parameters did not improve the RF regressor accuracy.

A challenge in ML training was to achieve high accuracy at channel location far from the entrance. Such challenge may arise in other problems if the flow is unsteady or in developing state. At a location where $n > 2$, h_n is determined by the overall upstream rib configuration, not just by a previous rib shape. Thus, as the number of upstream ribs increases, the determination of h_n becomes a more complicated problem since the number of parameters influencing h_n increases. Consequently, Fig. 3 shows that R^2 of h_n decreases, as n increases. This result also implies that the importance of features is not equal for the problem of h_n determination. For example, e_1 is considered the most important parameters among all e_n, since the first rib inevitably affects all other downstream ribs. On the other hand, e_4 and e_5 are of the least importance, as it is difficult for the fourth or fifth rib to be influential to other ribs. The RF algorithm quantitatively assesses how important each feature is on determining an arbitrary h_n. Relative feature importance score, evaluated by the RF algorithm, is 139 for e_1, 44 for e_2, 23 for e_3, and 1 for e_4 and e_5.

5. Interpolation

Interpolating capability of the ML regressor is investigated with new input data listed in Table 1. Ten different combinations of e_n were randomly generated where each combination contained at least one e_n that was not used in ML training. For each combination, mean absolute error of all h_n between FVM and ML regression was calculated, denoted as E_i. Fig. 4(a) shows one of the new channel geometries (case 2 in Table 1) and h_n of the corresponding design. Not only for case 2, but also for other new input data, h_n interpolated by the ML regressor were close to FVM predictions with E_i in the range of 10–65% and R^2 accomplished near 0.99. Note that a power function fitted to case 2 data,

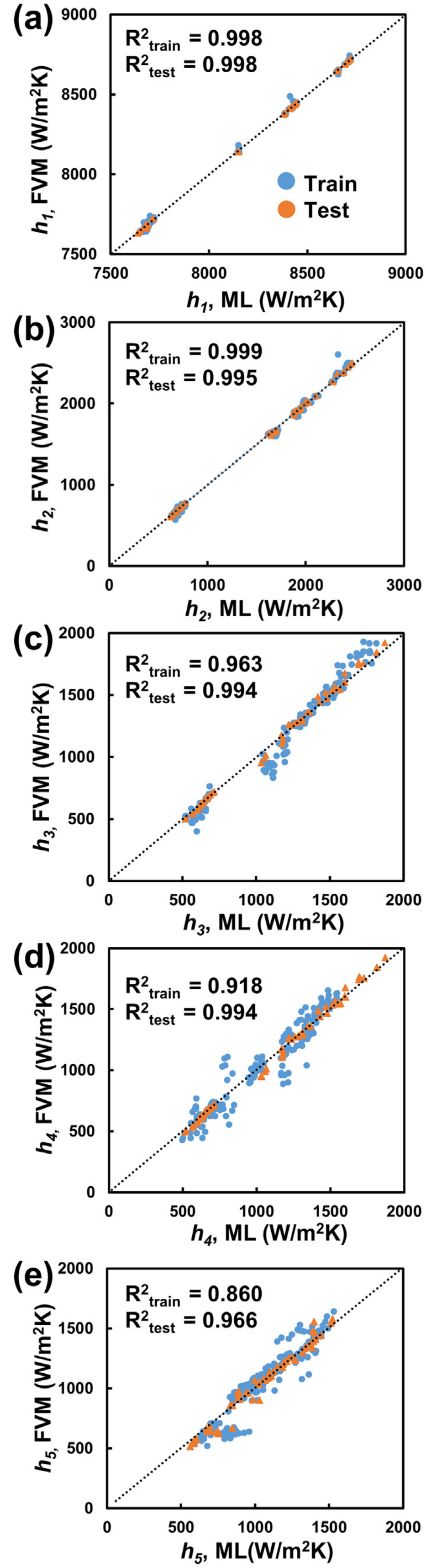

Fig. 3. Comparison of h predicted by FVM and ML regressor at (a) first, (b) second, (c) third, (d) fourth, and (e) fifth rib.

Table 1
Validation set. Inputs (rib heights, e_n) and results (mean absolute errors, E) of ML interpolation study.

Case	e_1 (mm)	e_2 (mm)	e_3 (mm)	e_4 (mm)	e_5 (mm)	E_i (%)	E_{re} (%)
1	0.1	0.2	0.3	0.4	0.5	34.5	8.0
2	0.5	0.4	0.3	0.2	0.1	64.0	11.2
3	0.0001	0.1	0.2	0.1	0.0001	12.5	12.1
4	0.0001	0.0001	0.5	0.0001	0.0001	39.8	34.7
5	0.1	0.5	0.8	0.4	1	27.9	19.2
6	0.31	0.95	0.03	0.43	0.38	24.9	16.6
7	0.76	0.79	0.18	0.48	0.44	35.7	6.5
8	0.64	0.70	0.75	0.27	0.67	24.3	18.4
9	0.65	0.16	0.11	0.49	0.95	29.7	14.8
10	0.34	0.58	0.22	0.75	0.25	26.7	5.9

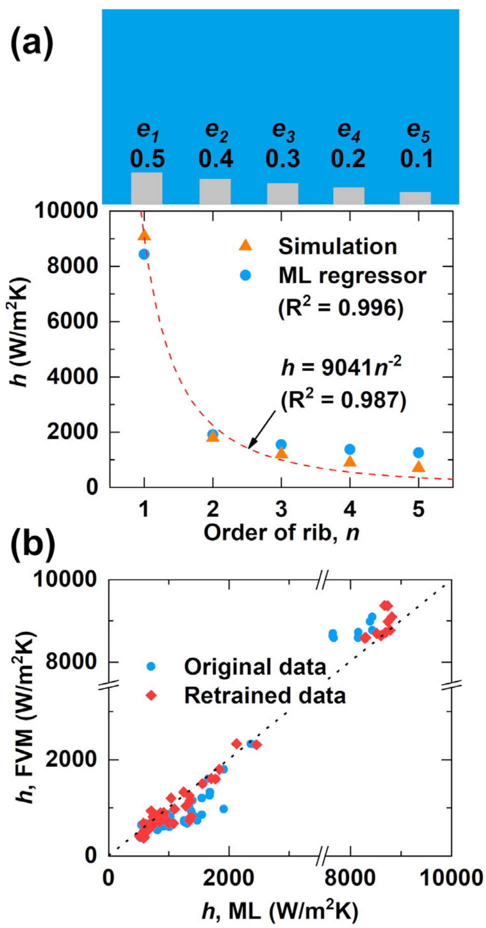

Fig. 4. (a) Comparison of h predicted by FVM and ML regressor for the channel geometries with [e_1, e_2, e_3, e_4, e_5] = [0.5, 0.4, 0.3, 0.2, 0.1] (mm). (b) Comparison of h_n of all channel geometries listed in Table 1, evaluated by FVM with original ML and retrained ML regressors.

$h = 9041n^{-2}$, resulted R^2 of 0.987. A big limitation of such power function is that it is not reliable if any modification of geometric parameters nonlinearly and drastically affects h. Compared to any simple mathematical-form correlation, a single ML regressor can be much more accurate especially for unsteady, nonlinear systems.

Although the ML regressor is able to interpolate the new dataset to a certain extent, its interpolation capability is limited unless sufficient data is provided. For example, in cases 1 and 2, e_n are in a similar range while the sequence of e_n values are reverse to each other. However, the ML regressor trained only by e_n = 0.0001, 0.1 or 1 mm was not able to differentiate these two cases, and generated the same h_n for the cases 1 and 2, leading to a significant E_i for case 2.

To readily enhance the accuracy of the ML regressor, new channel designs shown in Table 1 along with their h_n calculated by FVM were additionally added to the original training data. The addition of new data increased the number of training data from 182 to 192 (5.5% increment) and we retrained the ML model with updated dataset. The mean absolute error of all h_n between FVM and retrained ML regression was calculated, denoted as E_{re}, as presented in Table 1. Interestingly, such slight increase in data size meaningfully reduced the ML regressor errors. Mean square errors were also computed, which decreased from 2.9×10^5 to 1.9×10^5 through retraining. Fig. 4(b) compares h_n of all channel geometries listed in Table 1, evaluated by FVM with original ML and retrained ML regressors. Apparently, the predictions by the retrained ML regressor fits to FVM estimations better than the originally trained ML regressor. However, in cases 4,5, and 8 where the rib heights abruptly decrease between rib 3 and 4, the retrained ML regressor still exhibited overall E_{re} greater than 18%. This result implies how important it is to design the input features and training dataset for ML training. The ML algorithm can accurately predict for a variety of situations, if it is trained by well distributed input dataset. For instance, the input designs used in this study were the combinations of three e_n values. If the input designs incorporated more diverse e_n values, the ML regression would have been further accurate when interpolating for new channel geometries.

6. Conclusions

This work explored ML regression as a convection heat transfer correlation. A simple ML algorithm, random forests, was trained by numerical simulation data, and predicted the convection heat transfer coefficients, h, of cooling channels with variable surface roughness. Despite the high complexity and nonlinearity of h along the rough channel, a single RF model predicted closely to FVM calculations with R^2 > 0.860 for the training dataset and R^2 > 0.966 for the testing dataset, which has not been accomplished by any single mathematical-form correlation. For the new validation dataset, i.e. designs unseen during ML training, the RF algorithm was also able to predict h, similar to FVM with $R^2 \sim 0.99$ based on its interpolation mechanism. ML model was proven to be versatile, as refining the resolution or expanding the range of parameters became much simpler task relative to the traditional correlation development. For more precise prediction of refined regions, ML model was retrained by integrating new data into an original training data, which accurately predicted h of new channel designs. The demonstrated framework is widely adopted in various fields with high reliability, thus it can be extended to other heat transfer problems involving multiple variables and complex phenomena.

Declaration of Competing Interest

The authors declare that they have no known competing financial interests or personal relationships that could have appeared to influence the work reported in this paper.

References

[1] T.L. Bergman, A.S. Lavine, F.P. Incropera, D.P. Dewitt, Fundamentals of Heat and Mass Transfer, John Wiley & Sons, Inc., Hoboken, NJ, 2011.
[2] T.A. Rush, T.A. Newell, A.M. Jacobi, Int. J. Heat Mass Transf. 42 (1999) 1541.
[3] L. Goldstein, E.M. Sparrow, J. Heat Transf. 99 (1977) 187.
[4] R.L. Webb, R. Narayanamurthy, P. Thors, J. Heat Transf. 122 (2000) 134.
[5] B.J. Erickson, P. Korfiatis, Z. Akkus, T.L. Kline, Radiographics 37 (2017) 505.
[6] J. Bell, Machine Learning : Hands-on for Developers and Technical Professionals, John Wiley & Sons, Indianapolis, IN, 2014.
[7] W.D. Smart, L.P. Kaelbling, Proc. IEEE Int. Conf. Robot. Autom. 4 (2002) 3404.
[8] A.L. Beam, I.S. Kohane, JAMA 319 (2018) 1317.
[9] S.L. Brunton, B.R. Noack, P. Koumoutsakos, Annu. Rev. Fluid Mech. 52 (2020) 477.
[10] P.J. Kreitzer, M. Hanchak, L. Byrd, ASME Int. Mech. Eng. Congr. Expo. Proc, American Society of Mechanical Engineers (ASME), 2013.
[11] L. Joss, E.A. Müller, J. Chem. Educ. 96 (2019) 697.
[12] M.P. Brenner, J.D. Eldredge, J.B. Freund, Phys. Rev. Fluids 4 (2019) 100501.

[13] E.S. Rosa, R.M. Salgado, T. Ohishi, N. Mastelari, Int. J. Multiph. Flow 36 (2010) 738.
[14] M. Raissi, A. Yazdani, G.E. Karniadakis, Science (80-.) 367 (2020) 1026.
[15] S. Lee, D. You, J. Fluid Mech. 879 (2019) 217.
[16] G.M. Hobold, A.K. da Silva, Int. J. Heat Mass Transf. 134 (2019) 511.
[17] A. Baghban, M. Kahani, M.A. Nazari, M.H. Ahmadi, W.M. Yan, Int. J. Heat Mass Transf. 128 (2019) 825.
[18] H. Zhou, Y.C. Soh, X. Wu, Appl. Therm. Eng. 76 (2015) 98.
[19] K. Jambunathan, S.L. Hartle, S. Ashforth-Frost, V.N. Fontama, Int. J. Heat Mass Transf. 39 (1996) 2329.
[20] G.M. Hobold, A.K. da Silva, Int. J. Heat Mass Transf. 125 (2018) 1296.
[21] L. Breiman, Mach. Learn. 45 (2001) 5.
[22] F. Pedregosa, G. Varoquaux, A. Gramfort, V. Michel, B. Thirion, O. Grisel, M. Blondel, P. Prettenhofer, R. Weiss, V. Dubourg, J. Vanderplas, A. Passos, D. Cournapeau, M. Brucher, M. Perrot, É. Duchesnay, J. Mach. Learn. Res. 12 (2011) 2825.